Study of Electronic Properties and Optical Transitions in Silicon

DR. ASHOK KUMAR SINGH

Department of Physics, HNK Inter College, Ara (Bhojpur), Bihar – India

ashokkumarsingh781@gmail.com

ABSTRACT - In this present paper eigen functions computed in the local density approximation by the full-potential linearized augmented-plane wave or the linearized muffin-tin-orbital method supply the input for generating the Green function G and the screened coulomb interaction w. A missed basis is used for the expansion to w, consisting of plane waves in the interstitial region and augmented wave function products in the augmentation sphere-regions. The frequency dependence of the dielectric function is computed within the random phase approximation. We have applied the al electron Gw calculation for wurtzite zincoxide, The Gw calculation overestimates the screening effect for localized states such as the Zn 3d states, because for the random phase approximation and local density approximation band structure. Self consistent calculations are needed to improve the results. For a four atom system having localized 3d orbitals such as Wurtzite Zincoxide, we can complete the Gw calculation with 32k points in Brillouin Zone within 3 days. The Gw band gap of Zincoxide is smaller than experimentally obtained value.

Keywords: Eigen Functions, Brillouin Zone, Gw Calculation, Green Function.

I. INTRODUCTION

The wurtzite crystals are BeO, BN, SiC, A*l*N, GaN, InN, ZnO, ZnS, CdS and CdSe. All the crystals have the wurtzite structure as the stable phase except BN. But at high pressure, hexagonal BN may transform into the wurtzite structure. Hang and Ching presented the band structure of six of these wurtzite crystals plus 28 other semiconductors with 17 of them in the zinc blende structure using the orthogonolised linear combination of atomic orbitals method. However the calculations in that study were not self consistent and a minimal basis set was used. In the sprit of a semi-ab-initio approach, the exchange parameter in the one electron atomic like X-α potential was adjusted so as to reproduce the experimental band gap for each crystal. The semi-ab-initio approach with a minima basis set gave results far more superior than that semi emperical tight binding method with only a modest increase in computational effort. The transferability of the basis set and the potential makes of ideal for studying more complex configurations or for more demanding calculations such as non-linear optical properties.

The III-V nitrides AlN, GaN and InN and their alloys have prone sing application in semiconductor technology because of their larger band gaps in comparison with cubic III-V compound semiconductors[26]. A*l*N is also a very important ceramic material noted for its excellent mechanical thermal temperature resistant, and piezoelectric properties[27-28]. GaN has gained much attention recently because of its potential as a blue light emitter due to wider band gap. InN has been given very little attention because of material problems associated with defect contamination and other technical difficulties in the growth process. The application of II-VI compounds Zno, Zns, Cds, CdSe and their alloys in either Zinc blende or wurtzite structures are mainly in electro-optical and electro acoustic devices[29-30]. When doped with Mn, the Zn based wurtzite crystals to form an interesting group of dilute magnetic semiconductors.

Manabu Usuda and Noriaki Hamada[31] presented an all electron implementation of the GW approximation and applied it to wurtzite Zno. Eigen functions computed in the local density approximation by the full potential linearized augmented plane wave method supply the input for generating the green functions G and screened Coulomb interaction W. A mixed basis is used for the expansion of W, consisting of plane waves in the interstitial region and augmented wave function products in the augmentation sphere regions. The frequency dependence of the dielectric function is computed within the random phase approximation without a plasmon pole approximation. The calculated band gap is smaller than experiment by ~ 1 eV in constant to previously reported GW results.

 DOI : 10.35291/2454-9150.2019.0502 © 2019, IJREAM All Rights Reserved.

Density function theory provides a foundation for modern electronic structure calculations and the local density approximation is an efficient way to calculate the ground state properties of material. However, the local density approximation eigen values should not necessarily identified with the quasi particle energies, although eigen value differences are often used to describe the excited state. The G.W. approximation of Hedin[32] provides a practical method to calculate quasi particle energy. Hubertsen and Louie[33] presented the first G.W. calculation for real materials.

Several methods have been developed within various band structure calculation schemes[34]. Calculated quasi particle energies typically agree with experiment, for many kinds of materials. However, various kinds of approximation in addition to the GW approximation itself are usually employed, whose adequacy has been well tested. The local density approximation eigen functions generated by the full potential linearized augmented plane wave or a variant of the full potential linearized muffin-tin-orbital[35] methods, where in either case eigen functions are expanded in atomic like local functions in the muffin - tin sphere regions and in plane waves in the interstitial region. In order to treat the localized electrons accurately the Coulomb interaction V and the screened Coulomb interaction ω are expanded with a newly developed mixed basis that consists of two kinds of basis functions. One is the product basis functions developed by Aryasetiawan and Gunnarsson[36] which is constructed from the products of the local functions in the muffin tin sphere regions and equals to the usual plane wave in the interstitial region.

II. RESEARCH MODEL

2.1 LAWNICZAK-JABLONSKA, SUSKI, GOREZYCA ET AL MODEL

In this model they studied the electronic structure of group III nitrides A*l*N, GaN, InN and BN crystallizing in the wurtzite and graphite like hexagonal (BN) structures. A large set of the x-ray emission and absorption spectra was collected at the several synchrotron radiation facilities at installation offering the highest possible energy resolution. By taking advantages of the linear polarization of the synchrotron radiation and making careful crystallographic orientation of the samples, the bonds along axis and in plane in the wurtzite structure could be separately examined particularly for A*l*N they found pronounced anisotropy of the studied bonds. The experimental spectra were compared directly with ab initio calculations of the partial density of states projected on the action and anion atomic states. For the GaN, A*l*N and In N the agreement between structures observed in the calculated density of states and structures, observed in the experimental spectra was very good. In the case of hexagonal BN they have found an important influence of insufficient core screening in the x-ray spectra that influence the density of states distribution.

The x-ray absorption and emission measurements for lines with energy up to 600 eV were performed at the Lawrence Berkeley National laboratory. Advanced light source at the beam lines 6.32 and 8.0 respectively. In the case of x-ray absorption the total photocurrent measurement technique was applied for recording of the spectra. The energy resolution ΔE for the 1200 line/mm grating employed for nitrogen k edge was close to 0.16 eV. The Ga k-edge data were recorded using a Si (III) monochromator at the D-21 station, DCI ring, LURE and with higher resolution using the four crystalline Si monochromators in HASY LAB, station A*l*. At this station also the In L edge spectra were measured.

2.2 PRESENT MODEL

In my present model I have studied using the first principles orthogonalized linear combination of atomic orbitals method in the local density approximation, the electronic structures and the Linear optical properties of ten wurtzite crystals Beo, BN, Sic, A*l*N, GaN, InN, Zno, Zns, CdS and CdSc. Results on band structures density of states, effective masses, charge density distributions and effective charges were presented and compared. Optical properties of ten wurtzite crystals up to a phonon energy of 40 eV were calculated and the dielectric functions were resolved into components perpendicular and parallel to the z-axis. The calculated results were compared with the available experimental data and other recent calculations. The structural properties of the wurtzite crystals were also studied by means of local density total energy calculations. It is shown that the calculated equilibrium volume and the bulk models are in good agreement with recent experimental data.

The main objectives of this model is to have a comprehensive set of results obtained by a state of the art method that could be the basis for their studies in these materials. The semi-ab-initio approach with a minimal basis set gave results far more superior than the semi empirical tight binding method with only a modest increase in computational effort. The transferability of the basis set and the potential makes it ideal for studying more complex configuration of the semi conductor systems and compounds or for more demanding calculations such as non linear optical properties.

 DOI : 10.35291/2454-9150.2019.0502 © 2019, IJREAM All Rights Reserved.

Almost all of the tin wurtzite crystals are materials of increasing importance in modern technology. Beo is a pyroelectric material composed of very high elements BN and Sic are known for their superior mechanical properties that are especially valuable in high temperature applications. Although the stable phase of BN is the hexagonal phase and Sic has a number of polytypes with ZB being the most common one, the wurtzite phase is important in connection with stability in the epitaxial growth of thin films and in the structural phase transitions under pressure.

The Kohn-Sham form of the exchange correlation potential with Wigner interpolation formula for additional exchange effects were used. I have applied a full basis set consisting of linear combinations of atomic orbitals expressed as sum of Gaussian type orbitals. In the calculation the 3d orbitals of An, Ga and Se and the 4d orbitals of Cd and In were treated as valence orbitals. Extra orbitals corresponding to exicited states for each atom were included to ensure sufficient convergence in the basis set expansion. For the optical calculation, the real part of the frequency dependent inter band optical conductivity was evaluated first with all the optical transition matrix elements between the unoccupied valence bands and the occupied conduction bands.

III. ELECTRONIC PROPERTIES AND OPTICAL TRANSITIONS IN SILICON

Silicon is probably the best known semiconductor. It has been studied for more than 40 years. We found that the optimum basis set for the LCAO calculation consists of the atomic orbitals of Si (1s2s3s4s 2p3p3d). Here, the Si (4s 3d) are empty shells and are used to augment the basis set to account for charge redistributions in the solid environment. The electron band structure of Si, calculated with the optimum basis set, is shown in Fig. 1 without spin-orbit interaction, Fig. 1 shows that the top of the valence band is at the Γ point. The minimum of the conduction band is at a general point between Γand X. The calculated indirect band gap is about 1.02 eV, which is very close to the experimental value of about 1.14 - 1.17 eV. The calculated conduction band mini9ma are at $(2\pi/a)(0.79,0,0)$ and at the equivalent points, one along each cube edge. The effective mass of the n-type carriers at the conduction-band minimum is very anisotropic. The calculated transverse and longitudinal effective mass are, from the band dispersions in Fig. 1, $m_{nl} = 0.20 \pm 0.03m_o$ and $m_{nl} = 0.93 \pm 0.03m_o$, respectively.

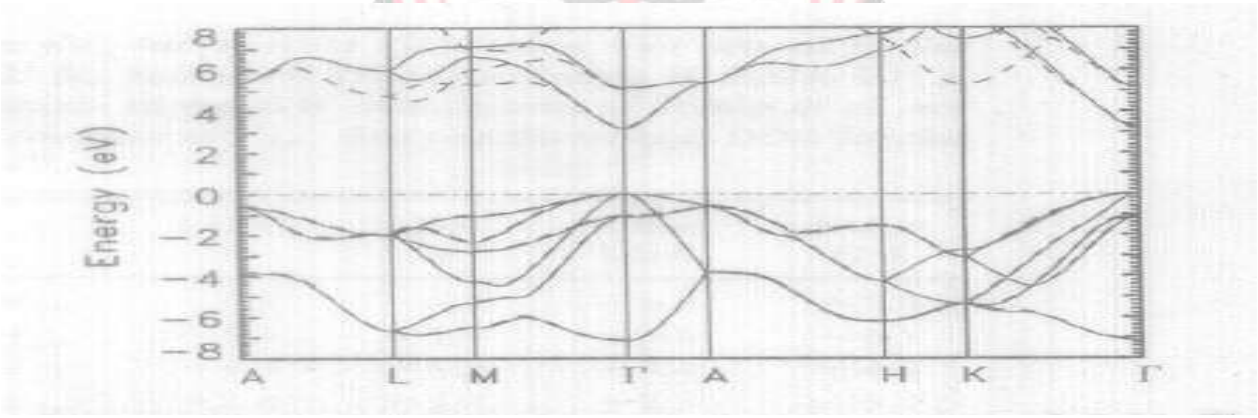

Fig. 1 - Electronic band structure of GaN.

Table 1. Comparison of the calculated interband-transition energies (in eV) for silicon (Si) with experimental results.

Si	This Calculation	Measurements
R_g	1.02	1.14[a], 1.17[b]
$\Gamma_{1v}\rightarrow\Gamma'_{25v}$	12.1	12.5±0.6[b]
$\Gamma'_{25v}\rightarrow\Gamma_{15c}$	2.68	3.0[c], 3.4[d]
$\Gamma'_{25v}\rightarrow\Gamma'_{2c}$	3.19	
$X_{4v}\rightarrow\Gamma'_{25v}$	2.93	2.9[e], 3.3±0.2[f]
$\Gamma'_{25v}\rightarrow X_{1c}$	1.26	1.3[b]
$L'_{2v}\rightarrow\Gamma'_{25v}$	9.80	9.3±0.4[b]
$L_{1v}\rightarrow\Gamma'_{25v}$	7.04	6.8±0.2[b]
$L'_{3v}\rightarrow\Gamma'_{25v}$	1.36	1.2±0.2[b]
$\Gamma'_{25v}\rightarrow L_{1c}$	1.66	1.65[g], 2.1[h]
$\Gamma'_{25v}\rightarrow L_{3c}$	3.78	3.9±0.1[b],4.15±0.01[i]

 DOI : 10.35291/2454-9150.2019.0502 © 2019, IJREAM All Rights Reserved.

$L'_{3v} \rightarrow L_{1c}$	3.0	3.2±0.2[b],3.45[d]
$L'_{3v} \rightarrow L_{3c}$	5.14	5.1±0.2[b],5.5[d]

These calculated effective masses are very close to the experimental values of $m_{nt} = 0.19m_o$ and $m_{nl} = 0.98m_o$. The good agreements between the calculated effective mass and the band gap, with corresponding experimental results, indicate that the lowest conduction band in Fig. 1 is reasonably reliable.

Table 1 shows the calculated interband-transition energies, along with experimental results, at selected critical points in the optical spectrum. In this table the indices *v* and *c* refer to the valence and conduction bands, respectively. The calculated optical transitions agrees well with experimental results. This agreement is particularly significant in light of difficulties in analyzing experimental data, including the effect of lifetime corrections. These corrections are expected to be significant for larger transition energies. In the experimental optical spectrum, each of the structures includes all possible optical transitions. The assignment of one structure to a particular transition from the experimentally measured optical spectrum has been a difficult problem in solid-state spectroscopy. The reported experimental $\Gamma'_{25v} \rightarrow \Gamma'_{2c}$ transition energy of 4.2 eV from the low-field electron-reflectance measurement, disagree with the calculated value of 3.19 eV. Our calculated data suggest that the 4.2 eV transition is rather the $X_{4v} \rightarrow X_{1c}$ transition energy. This conjecture is based on the following reasons.

(1) The small phase-space volume around the Γ'_{2c} point only contribute a tail-like structure to the density of states and to the optical spectrum.

(2) The Δ_5 and Δ_1 bands are nearly parallel for a substantial portion of the phase-space volume, increasing the possibility for mistake assignment of structures, and the calculated transition energies from X_{4v} to X_{1c} states are about 4.2 eV.

(3) The doubly degenerate Δ_1 bands have a spin-orbit splitting from the Γ'_{25} to the X_4 points, consistent with the experimental observations of the peak structures.

The $\Gamma_{1v} \rightarrow \Gamma'_{25v}$ transition is a measure of the valence band width. Our calculated valence-band width of 12.1 eV is in an excellent agreement with the experimentally measured value of 12.5 ± 0.6eV.

IV. BASIS SETS AND LATTICE PARAMETERS

It is important to note that the optimal size of the basis set for a given calculation varies with the nature and quality of the trial orbitals. Two computations for the same material, using Gaussian orbitals, are expected to lead to different sizes of the optimal basis set if the Gaussian exponents in the two calculations are different. The essential point is that both calculations must properly implement the procedure to arrive at the optimal size that applies, given the input orbitals. Further, Bagayoko showed that the use of contraction of orbitas leads to a rigid shift of the bands. This rigid shift does not affect the physics of the problem. It is a simple manifestation of the referenced variational. The bands obtained with contracted orbitals are shifted upwards as compared to those obtained with uncontracted orbitals - where the dimension of the matrices in the eigenvalue problem is larger.

The above points apply irrespective of the nature of the trial orbitals, i.e. Gaussian, exponential, or others, provided the increases in the size of the basis set progressively account for higher and higher energy orbitals of the input species (atoms or ions). In the case of plane waves, and in light of the relatively large number of orbitals, the implementation of the BZW procedure is expected to be more time consuming if plane waves are added or subtracted one at a time. Additionally, complications arise if higher and higher exponent plane waves are added, as done in some plane-wave calculations, as opposed to beginning with the highest exponents (representing lower, occupied states). The difficulties could be reduced by using augmented plane waves. The adequacy of the trial basis set sirectly affects the number of additions or subtraction of orbitals for the purpose of determining the optimal basis set for molecules, clusters, or solids. As in the case of Gaussian orbitals, a set of the trial functions describing the ground states of the affected atomic or ionic species is expected to be a good start.

Our choices for the lattice constants were dictated by two considerations. The first one stems from the fact that our program package does not yet include accurate codes for the calculation of the total energy. The search for equilibrium lattice parameters requires high accuracy. The second consideration, equally important, actually dictates that we utilize experimental lattice constants for some comparisons with measurements to be meaningful. Specifically, in the case of GaN, we considered two sets of lattice parameters to enable general comparison with experimental findings and specific comparison with the low-temperature results of Rubio et al. In case of silicon and diamond, matters are complicated further by the fact that some experiments reported slightly different lattice

 DOI : 10.35291/2454-9150.2019.0502 © 2019, IJREAM All Rights Reserved.

constants. While the use of experimental lattice parameters, as opposed to those for the minimum of the total energy curve versus the lattice parameter, is tantamount to applying pressure to a solid, the results discussed here are best fit for comparison with actual measurements.

V. RESULTS AND DISCUSSIONS

The self consistent pseudopotential method has been described in detail elsewhere. Self consistency here means the self consistent response of the balance electrons to a given structure of ions. In the present calculations, self consistent iterations continue until the screening potential is stable within 10^{-4} Ry together with the same degree of stability for the total energy. The local pseudopotential of Si used here is

$$U_{ps}(G) = a_1/G^2(\cos a_2G+a_3)e^{a_4G_4} \quad \ldots\ldots\ldots\ldots\ldots\ldots (1)$$

where a_1 = -1.1463 (for the bulk with a_c = 5.43Å), a_2 = 0.79065, a_3 = -0.35201, and a_4 = -0.01807, respectively. Rydberg atomic units are used throughout the paper. This pseudopotential for Si has been used successfully for various solid state calculations. The total energy per atom is

$$E_{total} = \Omega_{at}(\Sigma_{i,G} |\psi_i(k_i + G)|^2(k_i + G)^2 + 1/2 \Sigma_{G\neq0} V_H(G)\rho(G)$$

$$+3/4\Sigma_{G} \mu_{xc}(G)\rho(G) +\Sigma_{G\neq0} S(G)U_{ps}(G) \rho(G)) + \alpha_1 Z+\gamma E_{wald} \ldots\ldots\ldots\ldots\ldots..(2)$$

where Ω_{at} is the atomic volume, Z is the valency, the G's are reciprocal-lattice vectors, and S(G) is the structure factor. $\psi_i(k+G)$, $V_H(G)$, $\rho(G)$, $\mu_{xc}(G)$, and $U_{ps}(G)$ are Fourier transforms of the electron wave function, the Hartree potential, the total (valence) charge density, the exchange-correlation potential, and the local pseudopotential. The index i represents both the wave vector k_i and band index n and runs over occupied states of the valence electrons. α_1 and γE_{wald} are

$$\alpha = \lim_{G\to0}(U_{ps}(G)+8\pi Z/\Omega_{at}G^2) = 1/\Omega_{at}\int(U_{ps}(r)+2Z/ r)d^3 r, \ldots\ldots\ldots\ldots(3)$$

$$\gamma_{Ewald} = 1/2 \Sigma_{v} 2Z^2/|R_v| - 1/\Omega_{at} \int(2Z^2/r)d^3r \ldots\ldots\ldots\ldots\ldots\ldots\ldots\ldots..(4)$$

where the R_v's are lattice vectors to ionic sites. An alternative form for the total energy is

$$E_{total} = \Sigma_{v}\in i - \Omega_{at} (1/2 \Sigma_{G\neq0} V_H(G)\rho(G)+1/4\Sigma_{G} \mu_{xc}(G)\rho(G)+\alpha_1 Z+\gamma_{Ewald} \ldots..(5)$$

where the $\in_i$'s represent the eigenvalues of the valence electron wave functions. $\alpha_1 Z$ is calculated and shown in Table I for typical pseudopotentials of Si appearing in the literature. For non local pseudopotentials, the average of the s and p pseudopotential is given. Note that the choice of the local past from the nonlocal pseudopotentials is not unique as discussed in Rf. II.. Not all the pseudopotential derived from the atomic properties can be used in the momentum space formalism. For example, α_1 for the Simons-Bloch pseudopotential diverges (unless an artificial cutoff of the $1/r^2$ tail is introduced) because of the unphysically long-range character of the $1/r^2$ potential added to -2Z/*r*. The relatively large fluctuation of $\alpha_1 Z$ (1 Ry) among different pseudopotentials does not invalidate the pseudopotential scheme. For example, the pseudopotential

Table-2. Typical ionic pseudopotentials of Si. $\alpha_1 z$ is evaluated for these pseudopotentials (z = 4)

Reference	Pseudopotential	$\alpha_1 z$(numerical values in Ry; at ac = 5.43Å
SCLC[a]	$a_1/q^2[\cos(a_2q) + a_3]\exp(a_4q^4)$	1.433 17
AH[b]	$2/\Omega_{at}[-4\pi Z/q^2+(\pi/\alpha)^{3/2}v_1+(\pi/\alpha)^{3/2}(3/2\alpha-q^2/4\alpha^2)v_2]\exp(-q^2/4\alpha)$	0.990 60
FKc	$\begin{cases} -e^2/r\,(Z'-Q+Qe^{-\alpha r})+Z'e^2/r\,\exp[-\sqrt{(Q/Z)}\alpha r]+V_c\gamma^3/(2\pi)^{3/2}\exp[-\gamma^2r^2/2)] \\ 0, \quad r < r_c \end{cases}$	11.65293

 DOI : 10.35291/2454-9150.2019.0502 © 2019, IJREAM All Rights Reserved.

Ashcroft[d]	$U(r) = -2Z/r,\ r > r_c$ $V_0 \cos kr + C_0,\ r < r_c$	1.932 12
TH[c]	$U(r) = -2Z/r,\ r > r_c$ $-\Sigma A_l P_l,\ r < r_c$	?
Heine[f]	$U(r) = -2Z/r,\ r > r_c$	1.518 58
Simons[g]	$U(r) = -2z/r + \Sigma A_l P_l/r^2$	∞
Zunger-Cohen[h]	(first-principles pseudopotential)	1.932

used by Zunger and Cohen has a very strong repulsive core, hence, a large $\alpha_1 Z$, nut its major effect is a rigid shift of the band structure downward with respect to the average potential. Therefore $\Sigma_i \in_i + \alpha_1 Z$ is insensitive to the pseudopotentials used as long as they are not pathological. γ_{Ewald} is readily available in the literture. γ_{Ewald} S for representative structures normalized to one electron per atom are listed below :

$$\gamma_{Ewald}^{(diamond)} = -5.386\ 80 / a_c = -1.680\ 85/r_s \quad (6)$$

$$\gamma_{Ewald}^{(fcc)} = -4.584\ 88 / a_c = -1.791\ 75/r_s \quad (7)$$

$$\gamma_{Ewald}^{(bcc)} = -3.639\ 24 / a_c = -1.791\ 86/r_s \quad (8)$$

$$\gamma_{Ewald}^{(hcp)} = -3.241\ 87 / a = -1.791\ 68/r_s \quad (9)$$

$$\gamma_{Ewald}^{(white\ Sn)} = -5.524\ 08 / a = -1.773\ 02/r_s \quad (10)$$

where a_c is the lattice constant of the cubic system. c/a = $\sqrt{8/3}$ and 0.554 are assumed for the hcp and white Sn structures, respectively. Values for the diamond, fcc, and bcc structures are quoted from ref. 20 [γ(fiamond) can be calculated from the relation γ (diamond) = γ(fcc) + γ(bcc) - γ (sc) for the same a_c], and values for the hcp, white Sn, and the slab structure are calculated analytically.

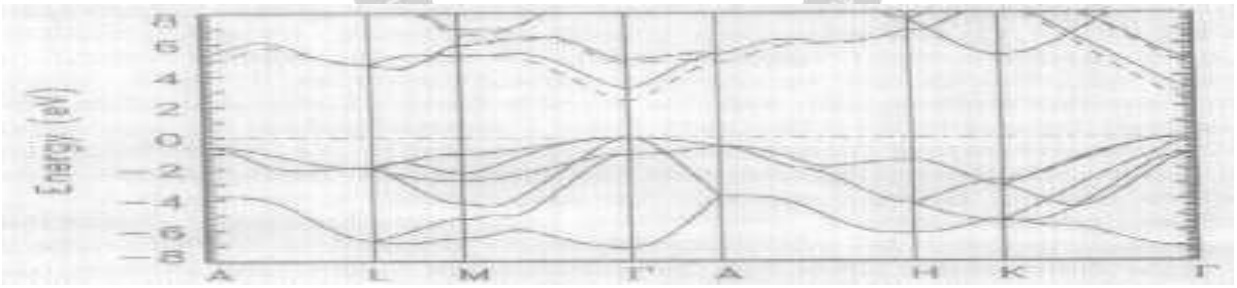

Fig. 2. Comparison of the results of calculation

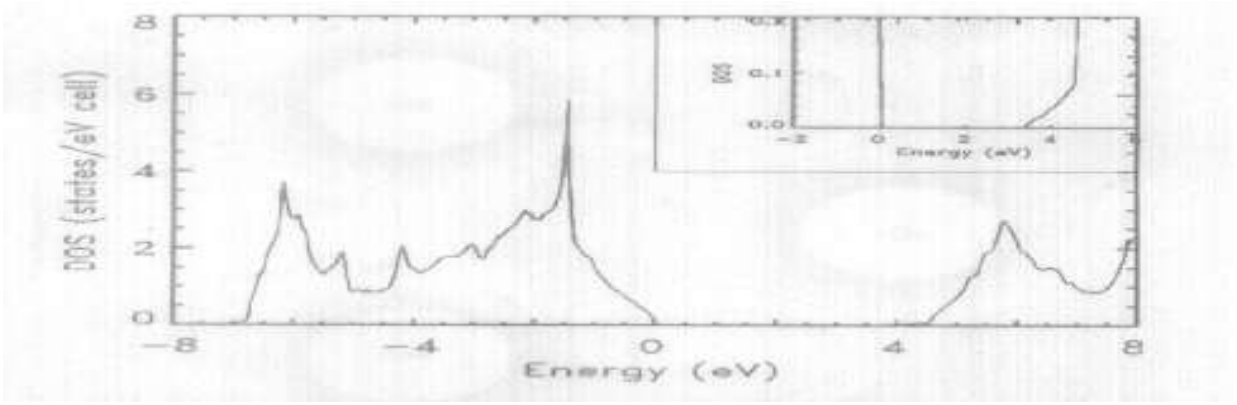

Fig. 3- The calculated density of states for wurtzite GaN.

 DOI : 10.35291/2454-9150.2019.0502 © 2019, IJREAM All Rights Reserved.

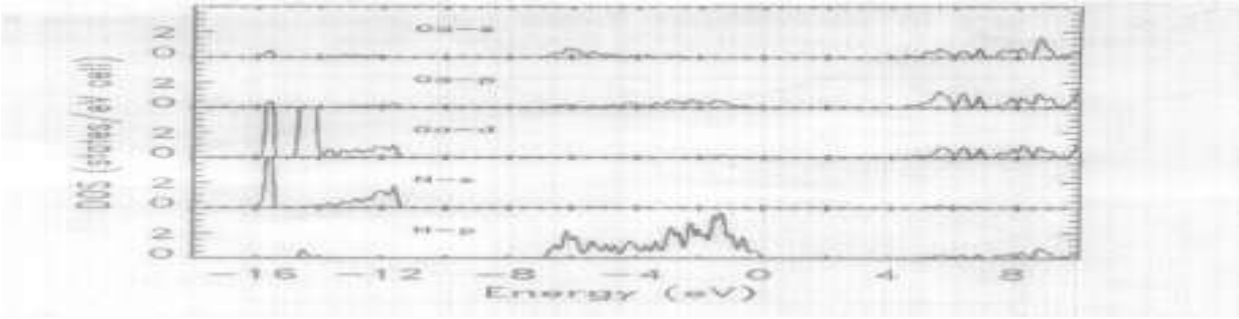

Fig. 4 - The PDOS for wurtzite GaN from the contribution of the s, p, and d states of Ga atoms and from the s and p states of N atoms.

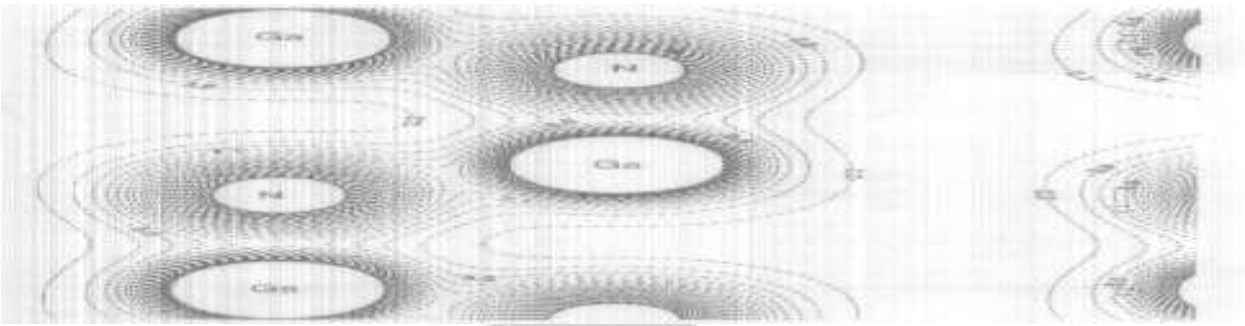

Fig. 5 - The charge density distribution on a (010) plane passing through Ga and N atoms. The lattice constants (room temperature) are a = 3.1878A, c = 5.1850A, and u = 0.375.

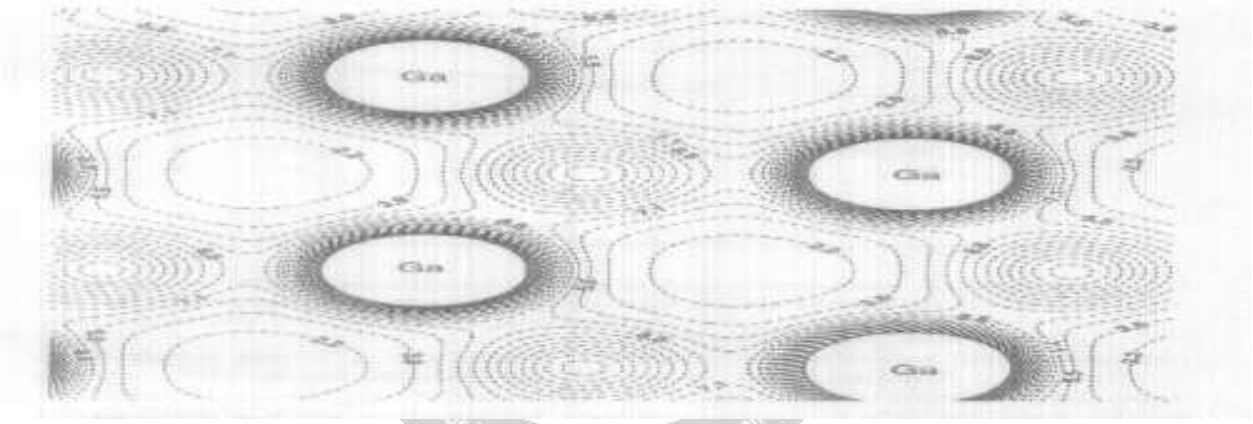

Fig. 6 - The charge density distribution on a (001) plane of Ga atoms. The lattice constants (room temperature) are a = 3.1878A, c = 5.1850A, and u = 0.375.

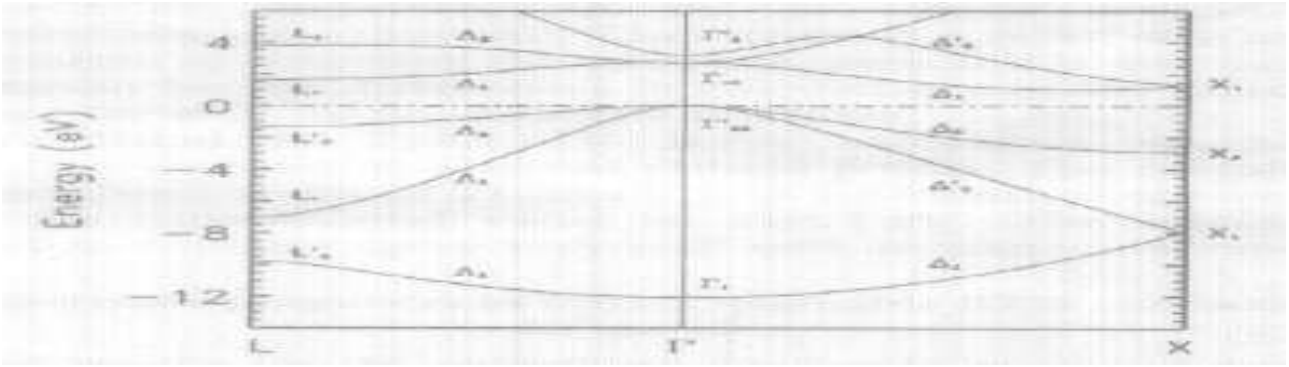

Fig. 7 - The calculated electron band structure of Si along the symmetry direction Λ and Δ, as obtained with the optimal basis set of the BZW procedure.

VI. CONCLUSIONS

This method has been successfully used for total-energy calculations to study the ground-state bulk properties in a number of crystals. Here, we report a similar calculation for the *W* crystals. As mentioned earlier, we assume a uniform scaling of lattice constants with the *c/a* ratio fixed, and calculate the total energy as a function of volume. In the total energy calculation, the accuracy of the fitted charge density must be maintained at a very high level. We have achieved in general a fitting accuracy of the

 DOI : 10.35291/2454-9150.2019.0502 © 2019, IJREAM All Rights Reserved.

order of 0.001 electrons per valence electron. We made no attempt to further optimize the fitting function. Our past experience and isolated tests indicate that the total energy result is not very sensitive to a minor variation in the basis function as long as a full bass set is used. It is conceivable that an improved result for total energy may be obtained by further optimizing the fitting function.

We made no attempt to improve the agreement by a selective choice of data points. Unfortunately, we are unable to locate the more recent experimental data for B and B' for several W crystals for comparison, and accurate experimental data for pressure coefficient B' for some crystals. As expected, the pressure coefficient B' is less accurate than B both experimentally and theoretically.

REFERENCES

[1] M.L. Cohen and J.R. Chelikowsky; Electronic structure and optical properties of semiconductors, (springer verlug, New York) (1988).
[2] E. Ghahramani, Phys. Rev. B, 41, 1542 (1990).
[3] J. Am Ceram, Soc. 71, 3135, (1990).
[4] J.C. Parker, U.W. Gelser, D.J. Lam, Soc. 71, 3206, (1990).
[5] D. Li etal Phys. Rev. B, 45, 5895, (1992).
[6] F. Gau, J.G. Harison, Phys. Rev. B, 45, 8248, (1992).
[7] Y.N. Xu and W.Y.Ching, Phys. Rev. B, 43,6159,(1991)
[8] R.N. French etal, ferroelectrics 111, 23, (1990)
[9] H. Jiang, Ferroelectrics 136, 137,(1992)
[10] M.A. Hasse, H. Cheng, D.K. Misemer, T.A. Strand and J. M. De Puydt, Appl. Phys. Lett. 59, 328, (1991).
[11] Manabu Usuda and Noriaki Hamada, Phys. Rev. B, 66, 125101 (2002).
[12] F. Aryasetiawan, In strong correlations in electronic structure calculations edited by V.I. Anisimov (Gordon and Breach, New York), (2000).
[13] M. Methdessed, M. Van Schilfgaarde and R.A. Casali, In electronic structure and physical properties of solids vol.-535, edited by H. Dreysse (Springer-Verleg, Berlin) (2000).
[14] V.J. Keast, A.J. Scott, M.J. Kappers, C.T. Foxon and C.J. Humphreys, Phys. Rev. B, 66, 125319, (2002).
[15] V.I. Gavrilenko and R.Q. Wu Appl. Phys. Lett. 77, 3042, (2000).
[16] Gorczyca, N.E. Christensen, K.A. Attenkofer R.C.C. Perera, E.M. Gulikson, J.H. Underwood, D.L. Ederer, Phys. Rev. B, 61, 16623, (2000).

 DOI : 10.35291/2454-9150.2019.0502 © 2019, IJREAM All Rights Reserved.